Progress In Electromagnetics Research M, Vol. 44, 101–108, 2015

Permanent Magnet System and Electron Gun Design for a 3rd Harmonic Peniotron

Xinhui Wu[1, *], Jianli Huo[1], Biao Hu[2], Jiayin Li[2], Jufen li[1], and Puchun Chen[1]

Abstract—This study discusses the operating characteristics of a large-orbit electron gun and a corresponding permanent magnet system of a 3rd harmonic peniotron. After optimization, a novel axis-encircling electron beam with axial velocity spread 4.48%, guiding centre deviation ratio 6.97% and high velocity ratio 2.03 is obtained. Driven by the electron gun, an output power of 35.4 kW is obtained, and the device efficiency is up to 56.0%, which is an attractive result in laboratories. The main advantages of such a peniotron are its compact size and low cost, which can meet the needs of vehicle, airborne and other mobile devices. The numerical analysis reveals that the relative axial position between the electrode system and magnet system has a great influence on the device performance, which needs careful control and precise adjustment.

1. INTRODUCTION

All the gyro-devices, including small-orbit gyrotron [1–4], large-orbit gyrotron [5–7] and peniotron [8–11], use interaction between the transverse energy of cyclotron electron beam and transverse electric field of electromagnetic mode. Peniotrons have been proven capable of achieving high conversion efficiency [8]. However, the experimental progress of them was much lower than expected, and the main technology obstacle is the difficulty in the formation and modulation of high-quality axis-encircling electron beam.

We have reported an 8 mm-band 3rd harmonic peniotron in previous studies [9, 10]. In this paper, a corresponding permanent magnet system and large-orbit electron gun are designed, which can meet the special requirements of the beam-wave interaction in the above mentioned peniotron. The main advantages of such a peniotron are its compact size and low cost, which can meet the needs of vehicle, airborne and other mobile devices. The prominent feature of this magnetic system is its very short transition zone. Although a short transition zone helps reduce the volume, it also makes the electron gun design a challenge. Under the permanent magnetic condition, an axis-encircling electron beam with axial velocity spread 4.48%, guiding center deviation ratio 6.97% and high velocity ratio 2.03 is obtained. Finally, the electron gun with a gradually reversed magnetic field is used to drive the 3rd harmonic peniotron. An output power of 35.4 kW is obtained, and the device efficiency is up to 56.0%.

2. THE PERMANENT MAGNET SYSTEM

The gyro-devices typically operate in strong magnetic field as the operating frequency and electron cyclotron frequency required should be close to each other. In general, the strong magnetic field is provided by a large, bulky and expensive superconducting magnetic system. In plasma heating and other large systems [3, 4], the magnetic system has no problem, but for vehicle systems and small mobile devices it will become a serious obstacle. However, compared with the superconducting magnetic

Received 21 August 2015, Accepted 18 October 2015, Scheduled 23 October 2015
* Corresponding author: Xinhui Wu (xinhuiwu2004@126.com).
[1] School of Science, Southwest Petroleum University, Chengdu, Sichuan, P. R. China. [2] School of Physical Electronics, University of Electronic Science and Technology of China, Chengdu, Sichuan, P. R. China.

system, a permanent magnet system does not consume electric power, additional power supply, cooling or protection installation. Besides, its size and weight are greatly reduced, and the magnetic field it provides is stable, reliable and of long life. Therefore, to obtain an output power of several tens of kilowatts permanent packaging millimetre-wave source is a common pursuit of international peers [5–10].

The presence of a reverse magnetic field in the cathode region is the key to producing large-orbit electron beam [11–15]. As shown in Figure 1, the axial magnetic field can be divided into four regions. Region I is the electron gun zone, in which the magnetic field direction is opposite to those of the other three regions. The reversed magnetic filed should meet the production requirement of the corresponding electron gun. The field in the transition region II should be smooth enough with no sudden change. Region III is the beam-wave interaction zone and is homogeneous with certain length. The amplitude of B_0 is determined by the cyclotron devices' working frequency, and its length is determined by the specific tube. Region IV is the depressed collector zone with its amplitude decreasing gradually, which can improve the device efficiency further by collecting the remaining electron beam.

The typical cross-sectional configuration of the 3rd harmonic peniotron is shown in Figure 2, and its basic characteristics are listed in Table 1, from which we propose the following requirements for the permanent magnet system. Firstly, the homogeneous magnetic amplitude of the beam-wave interaction region is about $B_0 = 0.396$ T. Meanwhile, it should have 5% adjustable. Secondly, to facilitate the sufficient beam-wave interaction in the resonator, and the homogeneous length should be 40–50 mm. Thirdly, to produce the required axis-encircling electron beam, the mutual adaption between the electron gun and the magnetic distribution of the cathode reversal region is very important. Fourthly, to facilitate the gun arrangement, the magnetic shielding can be added to the gun area.

The magnet design should be compact enough, and the magnet size, weight and cost should be taken into account. The permanent magnet system consists of permanent magnets, adjustable coils, and pole pieces. Its cross-sectional diagram is shown in Figure 3. Here, the NdFeB-32-MGOe is chosen as the permanent magnet material to provide the main field as it has good performance of magnetism, good mechanics, and its resources are rich enough compared with its predecessors [16]. The weight of the permanent magnets is about 26.6 kg, inner radius 120 mm, outer radius 230 mm and width 55 mm. The material of pole piece is A3 steel, and its total weight is 40 kg. An adjustable 8 kg magnet wire package is laid in the center of the magnet system to fine-tune the magnitude and the gradient of the field in the interaction region, which can strengthen the beam-wave interaction further. Coupled with

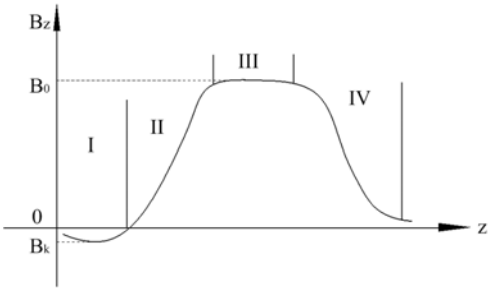

Figure 1. The axial magnetic field distribution of peniotron.

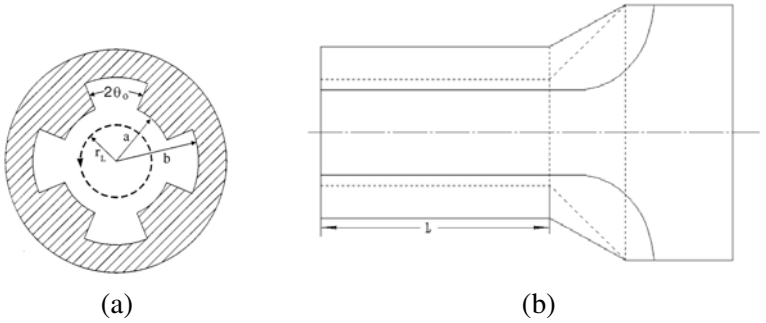

Figure 2. The cross sections of four-slotted peniotron model: (a) transverse and (b) longitudinal.

Table 1. Parameters of the 8 mm 3rd harmonic peniotron.

Voltage U/kV	43.5	Current I/A	1.45	Magnetic field B_0/T	0.396
Frequency f/GHz	30	Slot number N	4	Working mode	2π
Axial mode number	1	Slot ratio b/a	2.42	Inner radius a/mm	2.1
Cavity length L/mm	50	Loaded Q value	806	Cyclotron radius r_L/mm	1.62

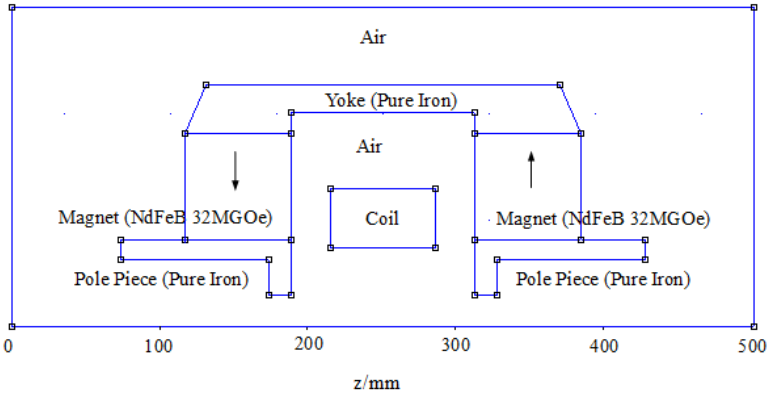

Figure 3. The cross-sectional configuration of the magnet system.

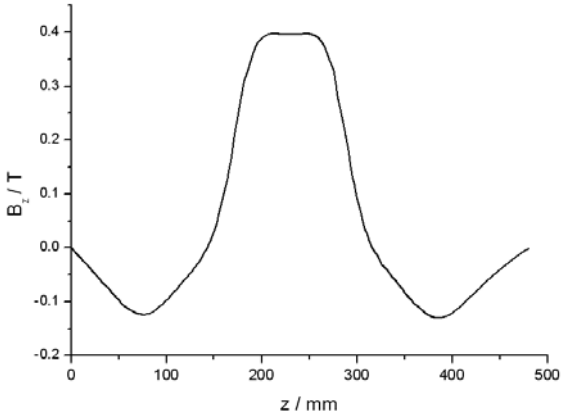

Figure 4. The magnetic field distribution along the system axis.

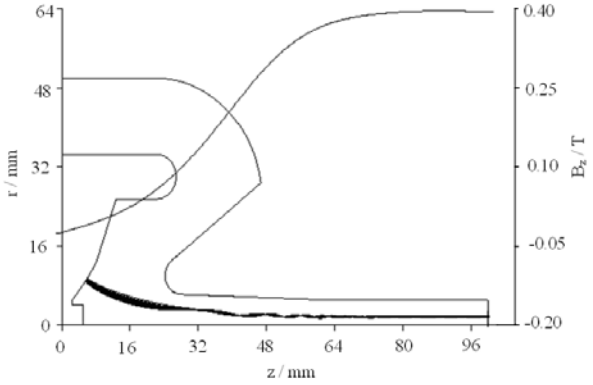

Figure 5. The gun structure of the 3rd harmonic peniotron (the gun region).

the other structural piece, the total weight of the magnetic system is within 100 kg. The axial length of the whole magnetic system is 500 mm, and the diameter is 300 mm. Obviously, its structure is very compact.

Figure 4 shows the axial magnetic field distribution along the system axis, from which we can see that the magnitude of the magnetic field uniform region is 0.396 T, and the length is about 50 mm. Within this range, the magnetic field inhomogeneity is less than 0.5%. Note that the distance from the reversal point to the entrance of the magnetic field uniform zone is only 70 mm, and it is a major problem for the electron gun design as to how to achieve axis-encircling electron beam conversion in such a short distance.

3. THE LARGE-ORBIT ELECTRON GUN

The performance of the electron gun is of paramount importance for the devices' overall efficiency. The optimized novel large-orbit electron gun together with the gradual reversal of the magnetic field and electron trajectories is shown in Figure 5. Here, the electron optics software EGUN is used to design the electron gun, and the field required is produced by the above-mentioned permanent magnetic system [17]. After optimizing the design, a practical novel large-orbit electron beam with axial velocity spread 4.48%, guiding centre deviation ratio 6.97% and high velocity ratio 2.03 is obtained. Distinguishing feature of such an electron gun is that our design does not pursue the formation of thin tubular electron beam and the utilization of mutation reversal magnetic field. It uses a gradual reversed magnetic field instead

of an abrupt one to form an axis-encircling electron beam, which reduces the difficulties in structure complexity and tube-making process. And the electrode configuration is not very sensitive to fabrication tolerances and allows for easy adjustment. The cathode emission band is placed in a divergent magnetic field before the magnetic reversal point rather than in a convergent one, and there is a distinct angle between the beam trajectories and magnetic field line. In the simulation, we find that the locations of the electrodes are a compromise between many contradictory conditions. In addition, by controlling the angular momentum difference between trajectory starting points and using the offset effect of various unfavorable factors, the guiding centre deviation ratio and velocity spread of the beam will be reduced greatly.

Both the particle in cell (PIC) simulation and the large signal theory of peniotron point out that the velocity spread and guiding center deviation ratio of the beam are the main factors affecting its performance [10, 18]. Whether the velocity spread is too large or the guiding center deviation ratio is out of control, it will cause the reduction of the device efficiency and the decline of the output power. The results of the electron gun and the basic requirements of the 3rd harmonic peniotron are shown in Table 2. As can be seen by comparson, the set of beam parameters fully meet the requirements of the 3rd permanent magnet packaging peniotron.

According to the simulation of large signal code of peniotron [10], an output power of 35.4 kW is obtained, and the device efficiency is up to 56.0% driven by the above-mentioned electron gun. Figure 6 indicates the distribution of relative electron beam energy along the z-axis. As shown in the figure, the energy of all electrons decelerates from an overall perspective (the electron energy at the outlet is smaller than that at the inlet), and the beam's remaining energy is relatively concentrated after through the interaction region, which is easy to collect by depressing collector further.

Table 2. Comparison of beam parameters between electron gun and peniotron.

Target	Beam requirements of peniotron	Results of electron gun
Working voltage/kV	43.5	43.5
Working current/A	1.45	1.45
Working magnetic filed/T	0.396	0.396
Velocity ratio	2.0	2.03
Velocity spread	$< 5\%$	4.48%
Velocity ratio spread	$< 10\%$	5.77%
Beam eccentricity	$< 10\%$	6.97%

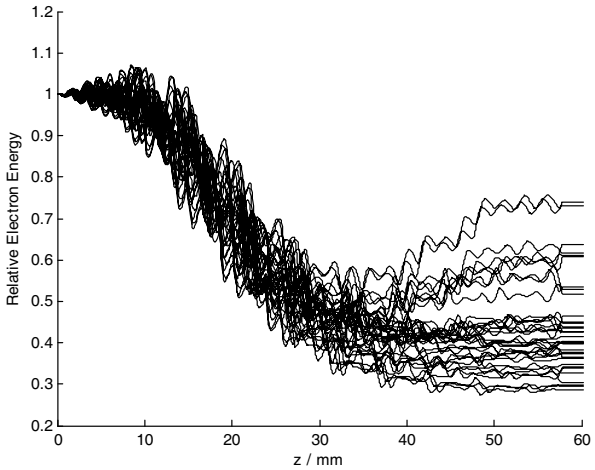

Figure 6. The distribution of relative electron energy (the interaction region).

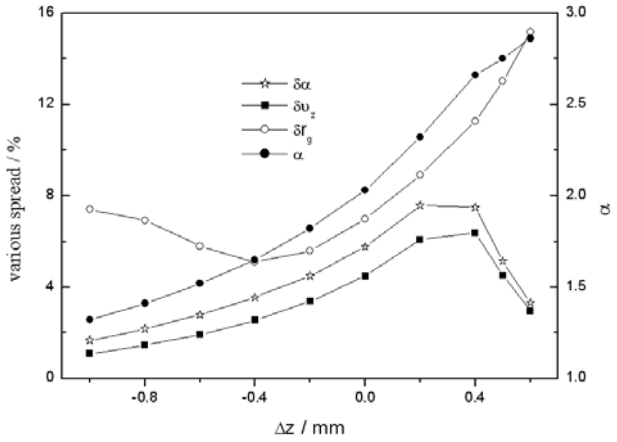

Figure 7. Beam performance vs. Δz.

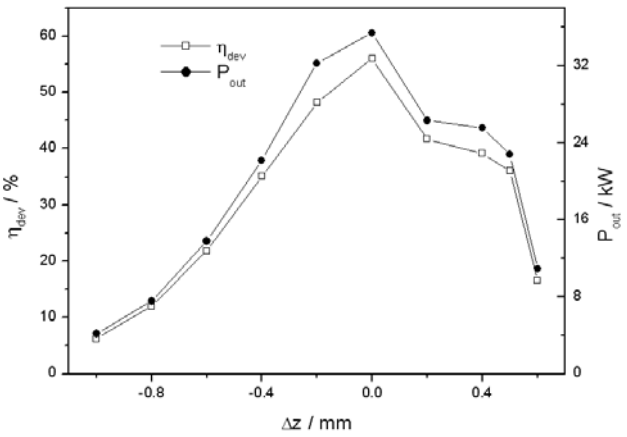

Figure 8. Device performance vs. Δz.

In the regulation of the electron gun we found that the electron beam quality is very sensitive to the relative position between the electrode system and magnetic system Δz, so it is bound to influence the performance of peniotron. The variation of the beam performance and device performance versus Δz are summarized in Figure 7 and Figure 8, respectively. In fact, the translation of the magnetic system relative to the electrode is equivalent to the change of the magnetic field strength B_k of the cathode region. As can be seen from the two figures, the cathode magnetic field B_k increases as Δz increases from -1 mm to 0.6 mm (the magnetic system pan right), and the velocity ratio is increasing, but the velocity ratio spread and velocity spread increase at first and then decrease, so do the output power and device efficiency. This is because the output power and efficiency are not determined by the velocity ratio uniquely, and they also have relationship with the degree of velocity spread and the guiding centre deviation ratio, which confirms our previous conclusion once again [10]. Specially, when the magnitude of magnetic field in cathode region increases to a certain value, that is, when the magnetic system shifts to the right to a certain extent ($\Delta z \geq 0.4$ mm), some electrons will reverse back to bombard the cathode. The more rightward shifting is, the more inversion electrons are. When the magnetic system shifts to the right of 0.8 mm, all the electrons will reverse back, and there will be no electrons participating in the energy exchange from the beam-wave interaction, which is also a major factor leading to a sharp reduction of the device efficiency. Taking all these factors into consideration, the position $\Delta z = 0$ mm is chosen in the design, and then the device efficiency and power are as high as 56.0% and 35.4 kW, respectively, which reach the maximum.

Figure 9 shows the distribution of relative electron energy at $\Delta z = -0.6$ mm. Although the velocity spread of the electron beam is small, the large beam eccentricity and small velocity ratio (i.e., small beam transverse energy) result in a relatively small energy exchange. Thus its efficiency and output power are relatively low. The distribution of relative electron energy at $\Delta z = 0.6$ mm is depicted in Figure 10. The remaining energy of the electron beam is not focused for the large beam eccentricity, and there is a small part of the electrons basically not producing any energy. Although the velocity ratio is large enough (i.e., beam transverse energy is big), there are 62% of the electron beam inversed already which are not able to participate in the energy exchange process. This is the major factor that leads to the dramatic reduction of device efficiency and output power.

From above analysis we conclude that the relative position between the electrode system and magnetic system is of great influence on the beam performance, thereby affecting the beam-wave interaction in the resonator. That is, it puts forward higher requirements for the regulating mechanism, even if a 0.1 mm deviation is critical, which is a major reason for the low efficiency of peniotron in experimental studies. In addition, the electron gun design is very difficult for the transition region of the designed permanent magnet system is too short, and it brings forward strict demands for the regulating mechanism. But at least it proves a possibility physically, that we may design a permanent magnet packaging millimetre-wave source with tens of kilowatts. A number of specific technical issues

will be solved step by step in the following research, such as designing a new magnet of which the cathode magnetic field varies slowly with its axial position.

The demountable peniotron system with a permanent magnet packaging is shown in Figure 11. All the four main components, including the permanent magnet system, high-frequency structure, axis-encircling electron gun and output coupling system, are aligned along the system axial direction (i.e., the direction that the beam travels). The magnet system is used for providing the magnetic field of the entire system, including the reversed magnetic field of the cathode region in the electron gun, the operating magnetic field in the beam-wave interaction region and the magnetic field for the output system. The gun system is used for providing the axis-encircling large-orbit electron beam. The high-frequency structure is a four-slot magnetron structure, which is also the site of beam-wave interaction. As soon as the electron beam is modulated to the appropriate quality by the joint action of the electric and reversed magnetic field, it will transform its portable transverse energy gradually into the high-frequency microwave energy, and the microwave energy will be amplified. The output coupling system collects the remaining energy of the electron beam. The permanent magnet system is under construction currently. After its completion, the 3rd harmonic peniotron with a permanent magnet system can be tested based on our host-test platform for the gyrotron.

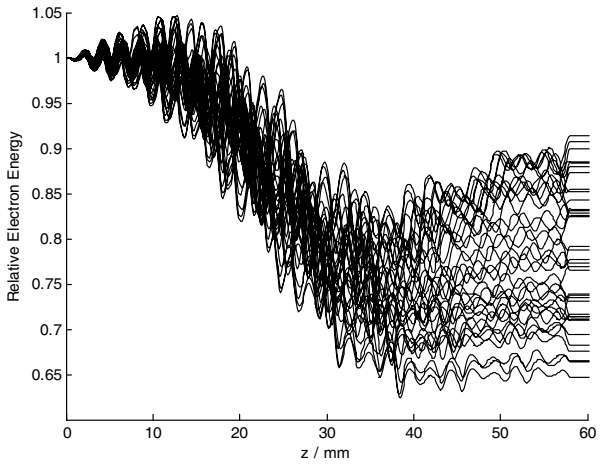

Figure 9. Distribution of relative electron energy at $\Delta z = -0.6\,\text{mm}$.

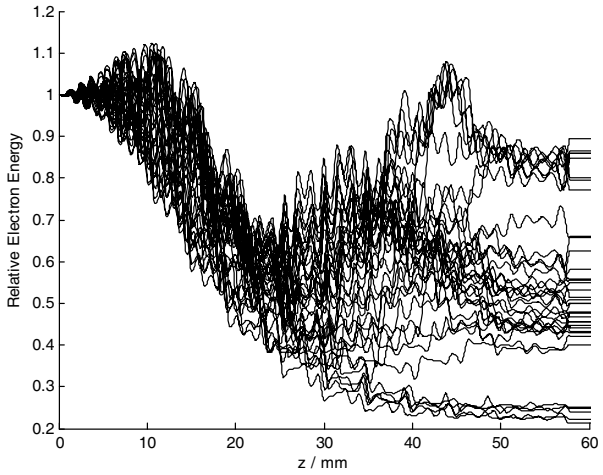

Figure 10. Distribution of relative electron energy at $\Delta z = 0.6\,\text{mm}$.

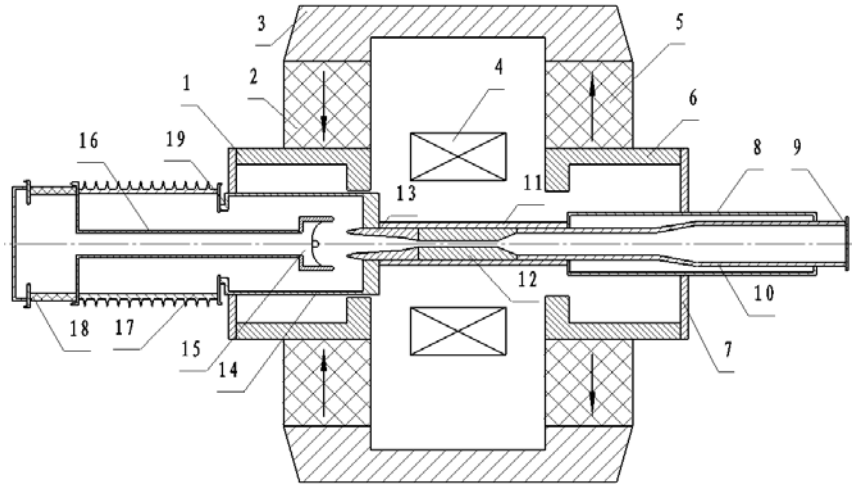

Figure 11. Profile of the permanent magnet packaging 3rd peniotron system.

4. CONCLUSIONS

This paper designs a large-orbit electron gun and a corresponding permanent magnet system of the 3rd harmonic peniotron, in which the existing conditions of magnet and feasibility of the technology are considered. A novel axis-encircling electron beam with axial velocity spread 4.48%, guiding centre deviation ratio 6.97% and high velocity ratio 2.03 is obtained, which can drive the 3rd harmonic peniotron. A high device efficiency 56.0% with output power 35.4 kW is obtained driven by the electron gun, which lays a good foundation for the development of permanent magnet packaging peniotron test systems. Such a peniotron with a permanent magnet system has two significant advantages. One is that the electron gun uses a gradual reversed magnetic field to form the axis-encircling beam instead of an abrupt field. The other is its much more compact size and lower cost. A particular note is that the relative axial position between the electrode system and magnet system has a great influence on the device performance, which needs careful and precise adjustment in the experiment.

ACKNOWLEDGMENT

This work was supported by the Department of Sichuan Provincial Education under Grant No. 14ZA0051, the School Foundation of Southwest Petroleum University under Grant No. 344 and No. 2012XJZ032.

REFERENCES

1. Singh, G. and B. N. N. Basu, "Modal analysis of azimuthally periodic vane-loaded cylindrical waveguide interaction structure for gyro-TWT," *Progress In Electromagnetics Research*, Vol. 70, 175–189, 2007.
2. Kumar, N., U. Singh, A. Kumar, H. Khatun, T. P. Singh, and A. K. Sinha, "Design of 35 GHz Gyrotron for material processing applications," *Progress In Electromagnetics Research B*, Vol. 27, 273–288, 2011.
3. Kesari, V., "Beam-absent analysis of disc-loaded-coaxial waveguide for application in gyro-TWT (Part-1)," *Progress In Electromagnetics Research*, Vol. 109, 211–227, 2010.
4. Kesari, V., "Beam-present analysis of disc-loaded-coaxial waveguide for its application in gyro-TWT (Part-2)," *Progress In Electromagnetics Research*, Vol. 109, 229–243, 2010.
5. Idehara, T., I. Ogawa, S. Mitsudo, Y. Iwata, S. Watanabe, Y. Itakura, K. Ohashi, H. Kobayashi, T. Yokoyama, V. Zapevalov, M. Glyavin, A. Kuftin, O. Malygin, and S. Sabchevski, "Development of a high harmonic gyrotron with an axis-encircling electron beam and a permanent magnet," *Vacuum*, Vol. 77, No. 4, 539–546, 2005.
6. Glyavin, M., S. Sabchevski, and T. Idehara, "Numerical analysis of weakly relativistic large orbit gyrotron with permanent magnet system," *Int. J. Infr. Mill. Waves*, Vol. 21, No. 8, 1211–1221, 2000.
7. Zapevalov, V., T. Idehara, and S. Sabchevski, "Design of a large orbit gyrotron with a permanent magnet system," *Int. J. Infr. Mill. Waves*, Vol. 24, No. 3, 253–260, 2003.
8. Vitello, P., "Design considerations for the gyro-peniotron oscillator," *Int. J. Infr. Mill. Waves*, Vol. 8, No. 5, 487–515, 1987.
9. Zhao, X. Y., J. Y. Li, and X. H. Wu, "Theoretical design and simulation of 8 mm-band third-harmonic slotted peniotron," *Chin. J. Vacuum Sci. Tec.*, Vol. 31, 194–200, 2011.
10. Wu, X. H., J. Y. Li, and B. Hu, "Numerical study of an 8 mm third-harmonic peniotron with a gradual reversal of the magnetic field," *Phys. Plas.*, Vol. 19, 023101-1-8, 2012.
11. Song, H. and T. Mulcahy, "A large orbit electron gun design for a terahertz harmonic gyrotron," *Journal of Electromagnetic Waves and Applications*, Vol. 25, No. 10, 1437–1447, 2011.
12. Zurk, L. M. and P. E. Serafim, "Relativistic electron motion in a resonant cavity with time varying and inhomogeneous magnetic fields," *Journal of Electromagnetic Waves and Applications*, Vol. 8, No. 1, 129–143, 1994.

13. Gallagher, D., M. Barsanti, F. Scafuri, and C. Armstrong, "High-power cusp gun for harmonic gyro-device applications," *IEEE Trans. Plas. Sci.*, Vol. 28, 695–699, 2000.
14. Hu, B., J. Y. Li, X. H. Wu, T. M. Li, and Y. H. Zhou, "Design of a large-orbit electron gun with gradual reversal magnetic field for a W-band permanent magnet peniotron," *Journal of Electromagnetic Waves and Applications*, Vol. 27, No. 9, 1136–1144, 2013.
15. Wu, X. H., J. Y. Li, B. Hu, and T. M. Li, "Generation of large-orbit electron beam using magnetron type injection gun," *Journal of Electromagnetic Waves and Applications*, Vol. 26, Nos. 14–15, 2070–2079, 2012.
16. Serrona, L., R. Fujisaki, A. Sugimura, T. Okuda, N. Adachi, H. Ohsato, I. Sakamoto, A. Nakanishi, M. Motokawa, D. Ping, and K. Hono, "Enhanced magnetic properties of Nd-Fe-B thin films crystallized by heat treatment," *J. Magnetism Magnetic Materi.*, Vol. 260, 406–414, 2003.
17. Herrmannsfeldt, W. B., "Egun-an electron optics and gun design program," Stanford Linear Accelerator Center, Stanford University, Stanford, California, 1979.
18. Kalyanasundaram, N. and P. Somaskandan, "Large-signal field analysis of an m-type travelling wave amplifier," *Journal of Electromagnetic Waves and Applications*, Vol. 7, 1355–1378, 1993.